ADVANCED FUNCTIONAL MATERIALS
www.afm-journal.de

Aerosol-Synthesis of Mesoporous Organosilica Nanoparticles with Highly Reactive, Superacidic Surfaces Comprising Sulfonic Acid Entities

*Julia Gehring, David Schleheck, Martin Luka, and Sebastian Polarz**

Combining high internal surface area with tailor-made surface properties is pivotal for granting advanced functional properties in many areas like heterogeneous catalysis, electrode materials, membranes, or also biomimetics. In this respect, organic-inorganic hybrid nanostructures and in particular mesoporous organosilica materials are ideal systems. Here, the preparation of mesoporous solids via a new sol–gel building block comprising sulfonic acid (R-SO_3H) is described. The degree of organic modification is not only maximal (100%), it is also proven that the novel material exhibits superacid properties. Furthermore, an aerosol assisted method is applied for generating this material in the form of mesoporous, spherical nanoparticles with substantial colloidal stability. Highly acidic, high surface area materials, like prepared here, are promising candidates for numerous future applications like in heterogeneous catalysis or for proton conducting membranes. However, first experiments addressing the antibacterial effect of the sulfonic-acid, mesoporous organosilica materials are shown. It is demonstrated that the superacid character is required for exhibiting sufficient antifouling activity.

1. Introduction

Biological evolution has created some of the most advanced functional systems known to date.[1] The precise knowledge about guiding principles of operation is pivotal for transferring concepts from biology to materials science and technology. The latter idea has led to the emergence of the seminal field "bionics", respectively biomimetics.[2] One of the most prominent cases is represented by the discovery of the construction principles for the lotus leaf and the resulting significant research activities on superhydrophopic surfaces and self-cleaning coatings in general.[3] The recognized paradigm is that solely the presence of certain chemical entities is not sufficient for granting a desired functionality, but the combination with micro-/nanostructured surfaces can be a decisive factor.

Therefore, in the introduction section of this article, we will firstly reflect on known methods for preparing high surface area materials furnished with tailor-made organo-functional groups. Secondly, we will discuss properties and potential applications of nanoporous materials comprising acidic functions. Furthermore, some contemporary approaches for antifouling materials as a special case of self-cleaning coatings will be addressed briefly.

1.1. Porous Organosilica Materials

The vast majority of inorganic solids comprising organically modified surfaces rely on silica chemistry. This is, because both Si–C and Si–O–Si represent two very stable linkages. The application of organosilane sol–gel precursors, for example, R-$Si(OEt)_3$ is an established technique for the preparation of various organic/inorganic hybrid materials, also known as ORMOSILs.[4] Huge activity in this field was driven by the development of novel techniques for nanostructuring, in particular the possibility to prepare periodically ordered mesoporous silica (POS).[5] A silica sol–gel precursor like $Si(OEt)_4$ is hydrolyzed at certain pH conditions and in the presence of a structure directing agent (template). Soon attempts were made to combine the areas POS and ORMOSILs.[6] Nice overviews were given by Ying et al.[7] in 1999 and Froeba and co-workers in 2006.[6] Starting from meso-SiO_2, via grafting or co-condensation using suitable organosilanes, one can achieve materials comprising up to 25% functionalization degree.[8] Much higher content of organic modification (up to 100%) accompanied by maximization of the density of the functional entities can be reached, when special sol–gel precursors with a bridging organic group R_f ($(R'O)_3S$-R_f-$Si(OR')_3$ with R′ = Me, Et, ^{iso}Pr) are used for the preparation of the so-called periodically ordered mesoporous organosilica materials (PMOs).[9] The organic functionality becomes an inherent part of the matrix. Since then, it has taken some time until PMOs with advanced chemical functionality could be realized. The interested reader is referred to one of the following, contemporary review articles.[10] Our group has concentrated on the so-called UKON

J. Gehring, M. Luka, Prof. Dr. S. Polarz
University of Konstanz
Department of Chemistry
D-78457, Konstanz, Germany
E-mail: sebastian.polarz@uni-konstanz.de
Dr. D. Schleheck
University of Konstanz
Department of Biology
D-78457, Konstanz, Germany

DOI: 10.1002/adfm.201302330

materials containing a bridging phenyl entity modified with various functional groups R in the 3-position of the aromatic ring:[11] R = –Br (≅ UKON-1), –COOH (≅ UKON-2a), $–NH_2$ (≅ UKON-2d), and so forth.

One important prerequisite for the application and future technological implementation of POS materials is the possibility to allocate processable samples. For this purpose, it is beneficial if a material of interest exists as a colloidal dispersion instead of an ill-defined powder. There has been some effort on the preparation of mesoporous silica in the form of colloidal nanoparticles. Two methods have been proven to be extremely powerful. One approach is a modification of the well-known Stoeber process.[12] Recently, Bein and co-workers presented monodisperse, mesoporous silica colloids with particles sizes in the 100 nm regime.[13a,b] It is also worth mentioning the papers by Jaroniec et al. and Froeba et al. about PMO nanoparticles generated via a modified Stoeber method.[13c,d] An alternative, highly innovative, aerosol assisted approach for the generation of mesoporous silica nanoparticles has been introduced by Brinker and co-workers in 1999.[14] Only few papers describe the preparation of PMO micro-/nanoparticles using bridging sol–gel precursors.[9c,15] To the best of our knowledge there is no report that reports about the synthesis of PMO nanoparticles via the aerosol-assisted route.

1.2. Porous Solid State Acids

Among the various functional groups, it has been shown that the preparation of mesoporous solid-state acids is of large interest, in particular for materials with strong acids like $–SO_3H$.[16] All current PMO materials comprising sulfonic acid have been prepared by post-functionalization routes. The direct sulfonation of a phenyl-bridged PMO was described by Inagaki et al. in 2002.[17] The proton-conducting properties of this material was reported very recently by Wark and team.[18] Kondo and co-workers used the Diels-Alder reaction for the attachment of an arylsulfonic acid to the π bond of an ethylene-bridged PMO.[19] Mehdi and colleagues could convert disulfide bridges to two terminal $–SO_3H$ functions in 2006.[20] There is currently no example for a PMO material with 100% sulfonic acid derivatization content, because this requires the availability of a $–SO_3H$ modified sol–gel precursor.

Furthermore, none of the reports mentioned above reports about superacidic properties of the respective, porous organosilica materials. The term superacid describes a system with an acidity greater (respectively a pK_a value smaller) than that of pure sulfuric acid.[21] The number of known solid-state superacids is yet quite limited. The most prominent examples involve sulfated zircona and some heteropolyoxometalate acids.[22] Also some zeolites exhibit superacid properties.[23]

There are manifold potential applications for acidic, and in particular superacidic, porous materials. They can act as heterogeneous catalyst materials for demanding organic transformations.[16b,24] Another interesting field is the application as novel proton conducting membranes for future fuel cells.[25] Furthermore, it is recognized that solid-state acids could potentially play a role also for self-cleaning surfaces.

1.3. Antifouling Materials

Microbial biofilms are very serious competitors for keeping surfaces clean and fouling of surfaces by microorganisms is a serious issue in many medical, biotechnological and food-technological settings, as well as in the shipping industry. In the recent years, a great deal of research has gone into finding novel chemical strategies (or biological strategies) for keeping surfaces clean. Furthermore, the demand for environmentally friendly approaches has increased significantly, since the ecological and toxicological issues of organotin compounds were taken much more serious.[26] An overview about chemical antifouling coatings and strategies was given by Kane and co-workers in 2011.[27] For example, a very promising approach comprises the photocatalytic activity of titania surfaces.[28] It is assumed that the photoreaction of TiO_2 with the solvent (e.g., water) is responsible for the generation of reactive species (e.g., H^+, $OH\cdot$), which then attack all organic species on the surface. It is also worth noting that the cytotoxicity of Ag^+ ions can be used, when silver nanoparticles are immobilized on surfaces via suitable anchoring groups.[29] Furthermore some hydrophilic polymers such as poly(ethylene glycol) (PEG),[30] polyoxazoline polymers,[31] and zwitterion-containing polymers such as poly[2-(methacryloyloxy) ethylphosphorylcholine (PMPC)[32] have been tested as effective coatings as they suppress protein adsorption.

Of special relevance for the present work are methods that involve chemical surface modification via silica sol–gel coatings.[33] For instance, Tang et al. describe the antifouling behavior of hydrophobic organosilica xerogels in 2005.[34] Furthermore, Mahltig et al. have demonstrated in 2008 that surface OH groups of wood can be facilitated for an attachment of organosilanes via sol–gel chemistry to exhibit antifouling properties.[35] Whereas the focus of these examples was on the hydrophobic nature of the surfaces, there is much less known whether materials may exhibit antifouling properties via active chemical triggers, such as strong acids like $–SO_3H$.

Herein, we report the synthesis of mesoporous UKON nanoparticles prepared via an aerosol aided synthesis route. Furthermore, a novel precursor comprising benzene sulfonic acid is presented. The precursor was used for the preparation of a highly acidic PMO material (UKON-2i). Finally, the UKON-2i nanoparticles were tested concerning a potential application in antifouling.

2. Results and Discussion

2.1. UKON Precursor and PMO Powder Preparation

The preparation of known sol–gel precursors and the related PMO materials containing bridging Ph-Br (UKON-1), Ph-CO_2H (UKON-2a), Ph-NH_2 (UKON-2d) is described in previous papers.[11] The pK_a value of benzoic acid is 4.3. This means that UKON-2a is expected to be a solid-state acid, but a rather weak one. Therefore, it would be highly desirable to have a PMO material available with much stronger acidity. Benzene sulfonic acid (Ph-SO_3H) is a promising candidate as a bridging organic

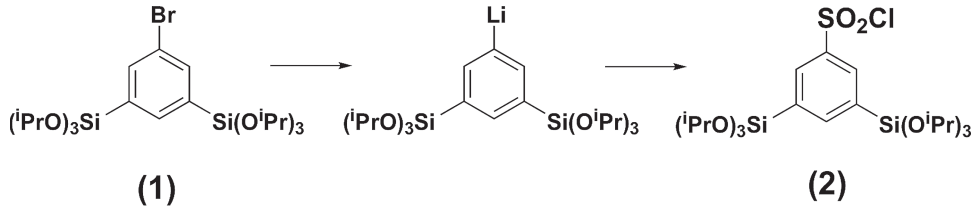

Scheme 1. Synthesis of the novel PMO precursor.

entity since its pK_a value is 0.7. In the current manuscript, we present the required, novel PMO precursor containing benzene sulfonic acid (Ph-SO_3H) and the preparation of the corresponding mesoporous organosilica for the first time.

In analogy to the other systems reported by us in the past,[11] the synthesis of the desired PMO precursor utilizes aromatic derivatization chemistry starting from compound (1) with bromine in 3-position (**Scheme 1**). Lithiation affords a stable nucleophile, which can react further with various electrophiles. Different attempts have been made for the introduction of the sulfonic acid group. An overview is given in the Supporting Information (S-1). Less successful were routes involving the oxidation of a thiol-functionalized compound, or the reaction of the lithiated species with SO_3. However, referring to the literature,[36] 1,5-bis-tri(isopropoxysilyl)-benzene-3-sulfonyl chloride (2) could be obtained in gram quantities using sulfuryl chloride as an electrophile.

Like for most sol–gel precursors, due to the influence of the alkoxy groups, it has not been possible to grow single-crystals for X-ray structure determination. The successful preparation and purity of (2) was proven by NMR spectroscopy (^1H, ^{13}C, ^{29}Si) and is documented in the Supporting Information, S-2. In addition, electron spray ionization mass spectrometry (ES-MS) was performed. The ES-MS pattern (given in S-2, Supporting Information) contains several fragmentation products, which can all be assigned to (2). The most intense signal and the simulated pattern for the corresponding fragment are exemplarily shown in **Figure 1**.

Next, the novel sol–gel precursor (2) was used for the preparation of PMOs referring to typical true liquid-crystal templating procedures reported in the literature.[37] Hydrolysis and polycondensation take place under aqueous conditions. Thus, it should be noted that in the case of compound (2) as a precursor not only the alkoxysilane groups react, but the S-Cl entity will also be hydrolyzed, yielding the desired sulfonic acid

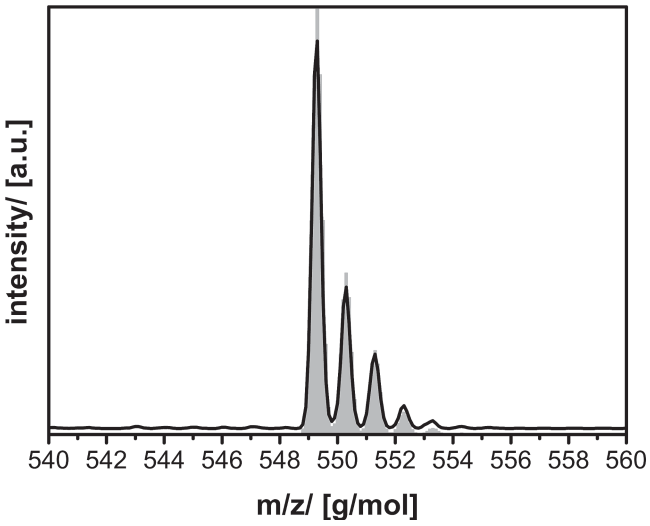

Figure 1. Excerpt from the ESI-MS pattern of (2) (black line) and simulated signal (grey) for the $[SO_2Ph(Si(O^iPr)_3)_2]^-$ species.

organosilica material (**Scheme 2**), accompanied by the formation of hydrochloric acid. The chemical nature of the resulting material was analyzed using a combination of techniques. First, solid-state NMR spectroscopy was applied. The ^{29}S-NMR spectrum (**Figure 2**b) contains characteristic three, so-called T-signals at $\delta = -65$ ppm for $(HO)_2R\underline{Si}(OSi) \cong T^1$, –73 ppm for $(HO)R\underline{Si}(OSi)_2 \cong T^2$ and –82 ppm for $R\underline{Si}(OSi)_3 \cong T^3$.[38] Q-type signals ($\delta \approx -110$ ppm) indicating the presence of pure silica (SiO_2) parts are absent. The latter result proves that the S–C bonds of the UKON precursor are stable during synthesis conditions.

Proving the presence of the $-SO_3H$ function is much more difficult. This is because sulfur is hardly accessible via NMR, and the chemical shifts of aromatic C's attached to $-SO_3H$ are

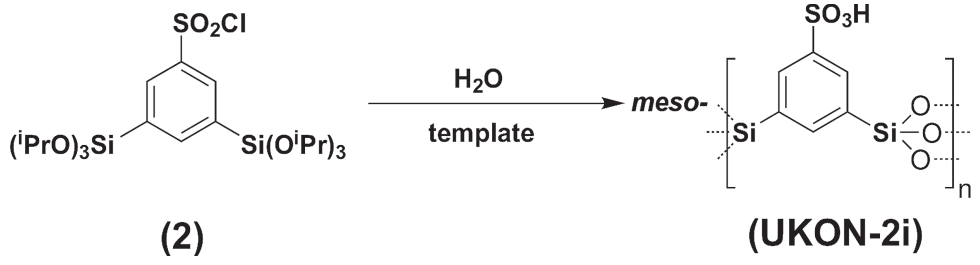

Scheme 2. Generation of the sulfonic-acid PMO material.

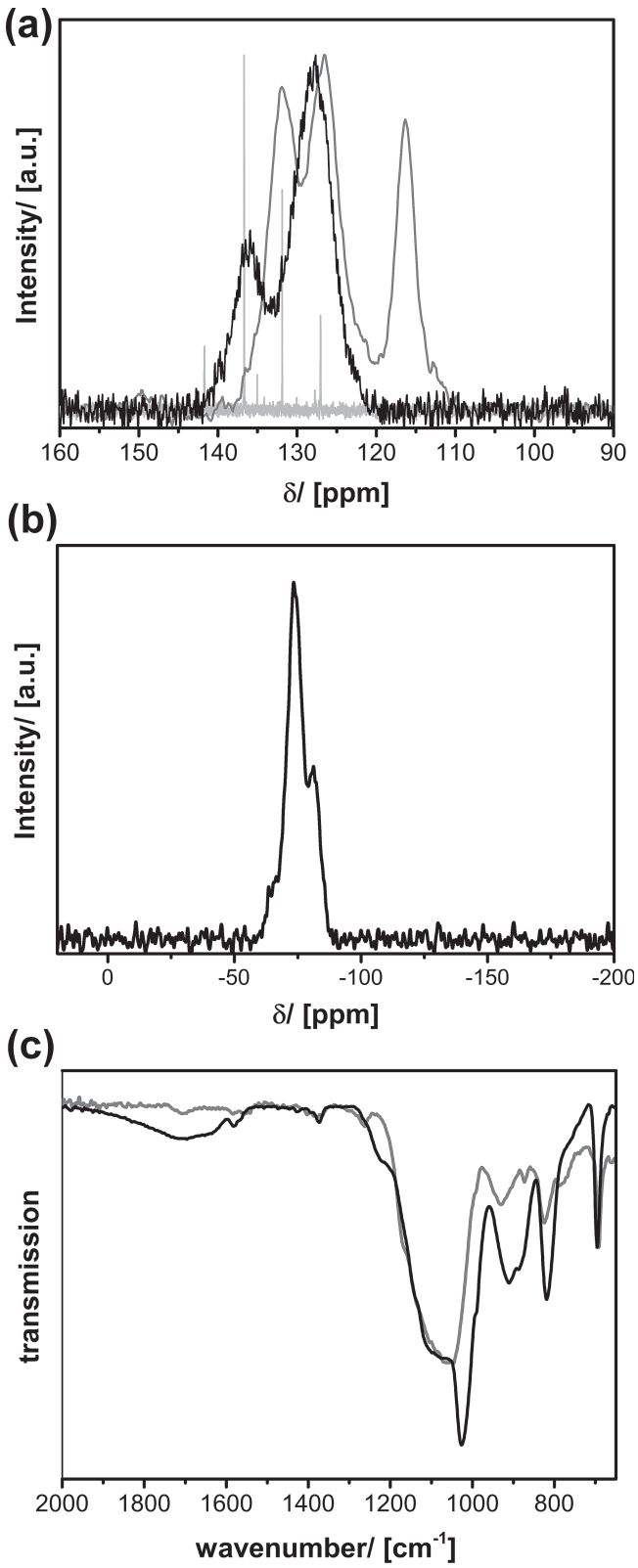

Figure 2. a) ^{13}C- solid-state NMR spectrum of UKON-2i (black graph) compared to the spectrum of UKON-1 (grey graph) and of the precursor (2; measured in solution; light grey graph) as references. b) ^{29}Si- solid-state NMR spectrum of UKON-2i. c) Fingerprint IR region of UKON-2i (black graph) compared to UKON-1 (grey graph) as a reference.

in a similar region ($\delta \approx 135$–140 ppm) as the signals of non-substituted or bromo-substituted aromatic rings.[11a,39] However, the direct comparison of UKON-2i to the NMR spectra of the precursor (2) and of UKON-1 (as a reference),[11a] shows good evidence that the sulfonic acid group is still present in the material. The signal at $\delta \approx 116$ ppm characteristic for C_{arom}-Br in UKON-1 is missing. Instead, a new signal can be found at 136 ppm, which is in good agreement to the NMR spectrum of the starting compound (2) (Figure 2a). Similar effects have been observed for IR spectroscopy (Figure 2c). In comparison to the spectrum of UKON-1, there is one additional band at 1024 cm^{-1} superimposed by the S–O–Si vibration of the matrix (1070 cm^{-1}). Comparison to information from the literature confirms that this new band can be assigned to the presence of the aromatic sulfonic acid.[40] In addition, energy dispersive X-ray spectroscopy (EDX) was performed (data given in S-3, Supporting Information). EDX shows that there is significant amount of sulfur present. The S:Si ratio equals 0.75:2, which is slightly less than expected (1:2), but still is within the error of the EDX method (±20%). Furthermore, X-ray photoelectron spectroscopy (XPS) was acquired (S-3, Supporting Information). The signal found at an electron binding energy of 169.1 eV is indicative for sulfur in oxidation state (+VI), in agreement to $R\text{-}S^{VI}O_3H$.[41] It can be summarized, that the sol–gel process has occurred as depicted in Scheme 2. The composition of the organosilica material can be described as $Si_2O_3(C_6H_3SO_3H)$. Neither C–Si nor C–S bonds were cleaved in course of the sol–gel process.

Successful meso-structuring of the sulfonic organosilica matrix required some unexpected, special measures described in the following. Initially, we chose a standard procedure which is well established for the synthesis of numerous PMO materials:[11] The precursor is dissolved in a solution of an amphiphilic, structure-directing block-copolymer of the Pluronic type in ethanol, and an appropriate amount of aqueous HCl (pH = 2) is added. Eventually pre-hydrolytic treatment is required (see experimental section). After polycondensation and drying one removes the template by liquid-liquid extraction. The characteristics of the pore system is studied by the typical set of analytical techniques used for mesoporous materials:[42] Transmission electron microscopy (TEM), N_2 physisorption measurements and small angle X-ray scattering (SAXS) if appropriate.

Other than expected, the physisorption isotherm (type I)[43] of the material prepared for those standard conditions is typical for microporous materials (**Figure 3**a). The latter result was confirmed by TEM micrographs (given in S-4, Supporting Information). Neither mesopores nor any ordered pore system can be identified. The reason for the missing structuration is that fragmentation of the PEO-PPO-PEO blockcopolymer (≅ Pluronic) into polyethylene oxide (PEO) and polypropylene oxide partitions has taken place. The latter was shown by time-dependent ^1H-NMR spectroscopy. The variances in the spectra (given in S-5, Supporting Information) are consistent with acid-catalyzed ether cleavage reactions. Once PEO and PPO are separated from each other, any amphiphilic property is lost and the formation of the liquid crystalline template is inhibited. Instead, the PEO chains lead to the formation of micropores.[44] The described result is a first indication for the enhanced reactivity of the sulfonic acid groups in UKON-2i.

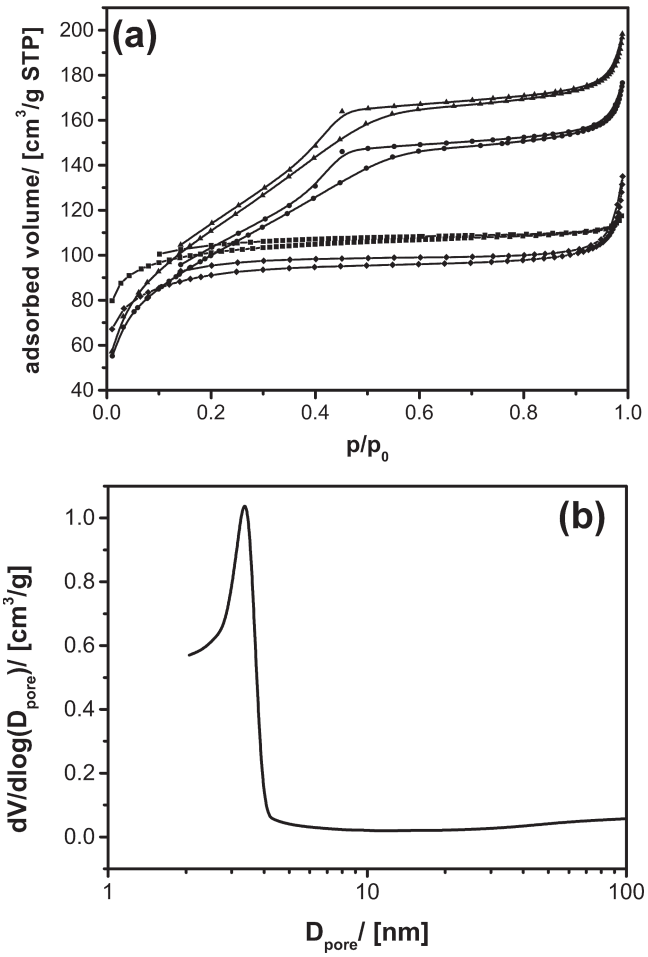

Figure 3. a) N_2 physisorption isotherms (adsorption and desorption) for UKON-2i materials prepared at standard conditions (squares), pH = 1.5 (circles), pH = 1.9 (triangles), and pH = 2.6 (hashes). b) BJH pore-size distribution of the UKON-2i material prepared at pH = 1.9.

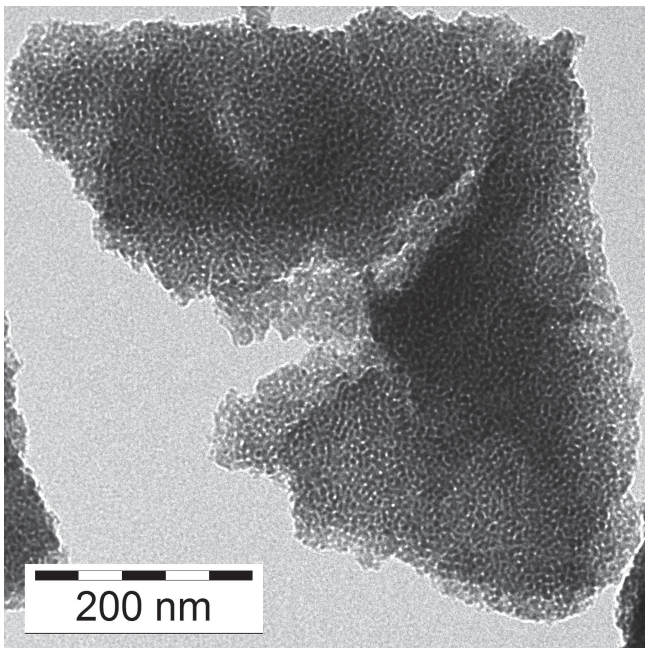

Figure 4. TEM image of UKON-2i prepared using Pluronic 123 as a template.

Because the hydrolysis of the S-Cl group in precursor (2) induces a significant drop of the pH-value, we checked, if control of pH using a buffer system leads to an improvement in structuring. Indeed, the emergence of an isotherm type characteristic for mesoporous materials (type IV), increased pore-volume and increased surface area (320 → 360 → 405 $m^2\ g^{-1}$) has been observed, when pH was adjusted to 1.5, respectively 1.9 (Figure 3a). The Barret, Joyner, Halenda (BJH)[45] pore-size distribution function is shown for the sample prepared at pH = 1.9 (Figure 3b). The observed pore-size of 3.5 nm is in the mesoporous range, but it is much smaller than for other mesoporous materials prepared using Pluronic P-123 as a template (D_{pore} = 5–6 nm). TEM investigation of the sample (**Figure 4**) shows that a mesoporous material has formed, in agreement to physisorption analysis. Unfortunately, there is a worm-hole type pore-system with low periodic order.

The subtle sensitivity of the UKON-2i system regarding pH value during synthesis can also be seen from the N_2 isotherm obtained for a material prepared at pH = 2.6 (Figure 3a). Again a type-I isotherm is seen, representing a microporous material. The difficulties in templating at higher pH values can be explained by the insufficient interaction between the neutral blockcopolymer template and the anionic -SO_3^- precursor species. It is known from the literature that it is preferred for successful templating using neutral block-copolymers, when the silica species are neutral as well.[46] It can be concluded that there is only a narrow pH window for the successful structuration of UKON-2i, when using Pluronics as structure directing agents.

Better results could be obtained for an amphiphilic poly[(ethylene-co-butylene)-b-(ethylene oxide)] (KLE; M_w = 8.1 kDa; 41% polyethylene oxide), due to its lower sensitivity towards proton catalyzed ether cleavage. KLE has already been applied successfully by others for the preparation of large-pore mesoporous silica and metal oxide materials.[47] TEM images of UKON-2i prepared with KLE as a structure directing agent (S-6, Supporting Information) show a highly ordered PMO material with an average pore size of ≈15 nm. The latter is in agreement with SAXS data, which indicate a periodicity of 17.2 nm (S-6, Supporting Information). The model used for the simulation of the SAXS pattern using the program package SCATTER[48] is shown in detail in S-6, Supporting Information. However, because KLE blockcopolymers are not commercially available, we still concentrate in the following on the application of Pluronics as templates.

2.2. Aerosol Synthesis of Colloidal UKON Nanoparticles

For the preparation of mesoporous organosilica materials in nanoparticle shape, we found that a modified Stoeber process cannot be adopted for the UKON system.[13,15e,49] This can be

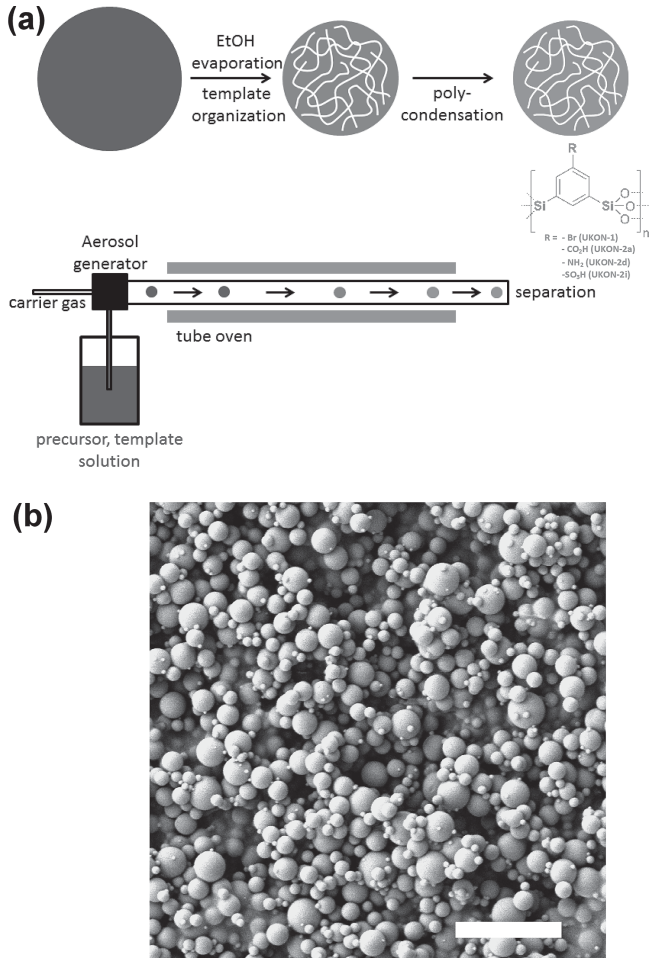

Figure 5. a) Illustration of the setup used for the preparation of mesoporous UKON-particles via an aerosol assisted process, and (b) SEM image of resulting spherical UKON-2i particles. Scale bar ≅ 2 µm.

attributed to two factors: The lower hydrolysis rate of the isopropoxysilyl groups (in comparison to ethoxy groups present in common sol–gel precursors) and the enhanced hydrophobicity of the precursor due to the aromatic ring hamper the growth of particles with defined porosity (results not shown).

Therefore, we have decided to test the aerosol-assisted method presented by Brinker et al.[14] A sol containing a prehydrolyzed UKON precursor, aqueous HCl, ethanol and an amphiphilic block-copolymer of the Pluronic type as a structure-directing agent is prepared (see Experimental Section). An aerosol containing small droplets of this mixture is prepared and is passed through a tube oven (**Figure 5**a). Ethanol evaporates, inducing liquid crystal formation due to the increased concentration of the polymer (evaporation induced self-assembly).[50] Polycondensation takes place, and the final mesostructured organosilica particles can be separated. Finally, after template extraction one obtains the desired mesoporous nanoparticles. Besides compound (2) (the precursor for UKON-2i; see Scheme 2), also the sol–gel precursors for UKON-1, UKON-2a, and UKON-2d have been used in analogous experiments in order to show the broad applicability of the method. Scanning electron microscopy (SEM) investigation shows that the samples contain numerous spherical particles in the size-range 100 nm–1 µm (see Figure 5b). The polydispersity is high, which is typical for particles obtained via aerosol routes.[51]

All materials were further characterized by TEM, SEM, N_2-physisorption analysis and solid-state NMR. This set of analytical data is summarized in S-7–10, Supporting Information. Exemplarily TEM images are shown in **Figure 6**. It is seen that all samples can be described as mesoporous materials with wormhole pore-system. The latter conclusion is supported by physisorption analysis (S-7–10, Supporting Information). The textural data (BET surface A_{BET} are and BJH pore-size distribution maximum D_{pore}) are summarized in **Table 1**.

It is important to note that the higher temperatures applied during the aerosol method (compared to the sol–gel process conducted in the liquid phase) does not lead to cleavage of the S–C bond, proven by the absence of Q-type signals in ^{29}S-NMR (data given in S-7–10, Supporting Information), and also not to detachment of the functional group in 3-position proven by ^{13}C-NMR, respectively by direct comparison to the corresponding data presented before for the (ordinary) powder samples.

2.3. Properties of Colloidal UKON-2i Nanoparticles

In the following, we emphasize some of the advanced properties of the spherical, mesoporous organosilica particles comprising the bridging benzene sulfonic acid entity (UKON-2i) (see also Figure 6d).

First, we tested if dispersions of those particles can be prepared in water. As the aerosol process affords also particles larger than λ_{vis} (= 400–800 nm) (see also Figure 7b), these dispersions appear turbid, which can be used to follow the sedimentation with the bare eye (**Figure 7**). Whereas conventional UKON powders (see above) sediment within seconds due to gravitational force, the effect is much slower for the porous nanoparticles prepared via the aerosol method. Furthermore, there is no flocculation. The latter observations represent good indication for the colloidal nature of the aerosol particles. The colloidal stability of the particles appears to be lower at low pH-values. A significant amount of particles have moved to the bottom of the vial within 100 min in a dispersion at pH = 1. This effect is reasonable, because the sulfonic acid becomes partially protonated (–SO_3H), which reduces the charge of the particles and hence leads to less electrostatic repulsion/stabilization. After 1000 min only the sample with pH = 9 still contains some dispersed particles. Similar effects can also be found for UKON-2a nanoparticles.

It is time to characterize the acidity of UKON-2i and in particular the related mesoporous nanoparticles in more detail. The results were compared to mesoporous UKON-2a nanoparticles with –COOH groups and pure SiO_2 nanoparticles as references. An established way for determining the acidity of solid-state acids beyond the Brønstedt window of water is to determine the Hammett acidity function H_0 by using appropriate indicator dyes (see Experimental Section).[52] In essence, one uses pH indicator dyes (D) with known pK_a values and investigates in organic solvents to what extend these dyes are protonated (DH^+) if the acidic substance of interest is present.

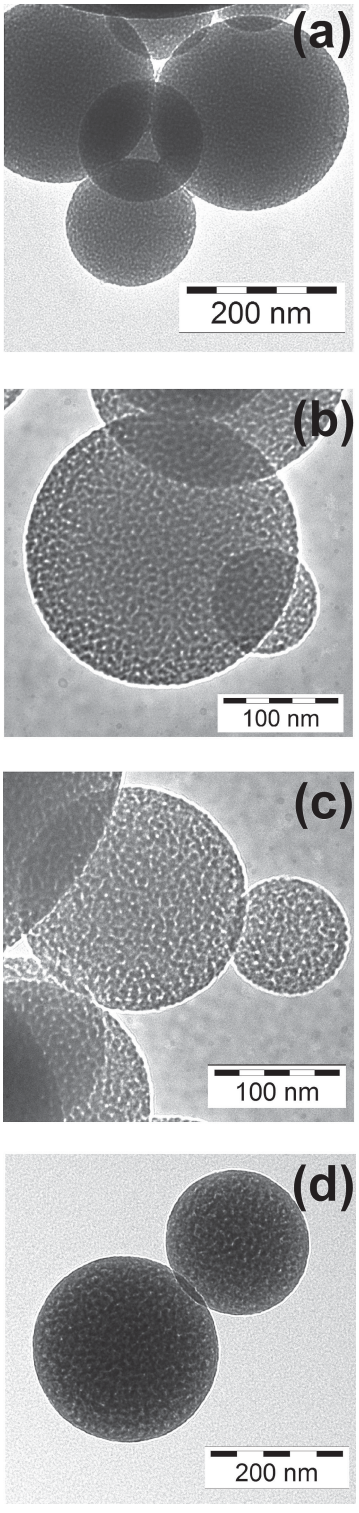

Figure 6. TEM images of mesoporous organosilica spheres prepared via the aerosol assisted method. a) UKON-1, b) UKON-2a, c) UKON-2d, d) UKON-2i.

$$H_0 = pK_a + \frac{c(B)}{c(BH^+)} \quad (1)$$

For determining the concentration of the protonated species $c(BH^+)$ and deprotonated species one facilitates optical measurements, followed by application of Lambert-Beer law. The measurements performed with 1-fluoro-4-nitrobenzene (FNB) (pK_a = –12.4) and 1-fluoro-2,4-dinitrobenzene (FDNB) (pK_a = –14.5) are shown in **Figure 8**. When UKON-2i is added to a solution of FNB one sees that its absorption band at λ_{max} = 256 nm drops in intensity due to protonation of the dye. This demonstrates that the acidity of UKON-2i is sufficient to protonate FNB to certain extend. Application of Equation 1 gives a value of H_0 = –12.53 for the Hammett acidity of the sulfonic acid containing PMO material. In comparison, the less basic FDNB cannot be protonated by UKON-2i. The spectra before and after addition of the PMO material are identical (Figure 8). It was mentioned before that sulfuric acid (H_0 = –12) represents an important reference mark. Therefore, one can conclude that

Table 1. Textural data for the mesoporous UKON spheres.

Sample	A_{BET}/ [m^2g^{-1}]	D_{Pore}/ [nm]
UKON-1_{100}[a)]	474	3.5
UKON-$2a_{100}$	424	4.1
UKON-$2d_{100}$	268	7.0
UKON-$2i_{100}$	720	3.5
UKON-$2i_{50}$	412	3.5
UKON-$2i_{10}$	550	3.8
SiO_2	635	5.5

[a)]The subscript indicates the organic derivatization degree. It is 100, if the bridging sol–gel precursor, e.g., compound (2) has been used in pure, undiluted form. Lower values indicate, that a mixture of the PMO precursor and $Si(OEt)_4$ ($\rightarrow SiO_2$) has been used during aerosol synthesis.

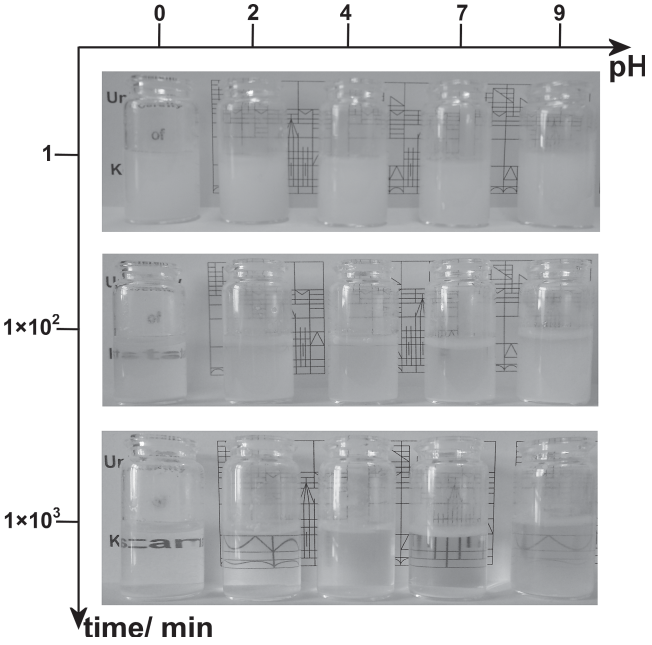

Figure 7. Photographic images showing the time-dependency of the sedimentation of UKON-2i nanoparticles as a function of pH-value.

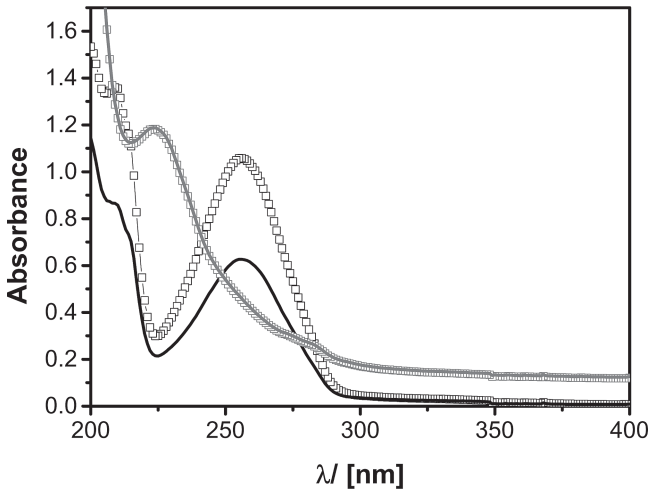

Figure 8. Optical absorption spectra of 1-fluoro-4-nitrobenzene before (black squares) and after exposure to UKON-2i (black line), and of 1-fluoro-2,4-dinitrobenzene before (grey squares) and after exposure to UKON-2i (grey line).

UKON-2i is slightly more acidic than H_2SO_4, and thus, belongs to the class of superacids. In comparison, UKON-2a ($H_0 = 2.38$); see S-11, Supporting Information) or unmodified mesoporous silica particles ($H_0 = 3.16$) are expectedly much less acidic. The results for UKON-2a concerning its weak acidity are in agreement with data obtained for tritration with 1 M NaOH performed in aqueous solution (see S-11, Supporting Information).

The amount of available protons per gram of UKON-2i nanoparticles, respectively per surface unit, can be determined via the ion exchange capacity (IEC); see also the experimental part.[53] The maximum IEC value can be obtained for UKON-2i nanoparticles prepared using the undiluted PMO precursor (UKON-$2i_{100}$; see **Table 2**).

The proton density can be calculated considering the surface area of the respective material (Table 1). The value obtained for UKON-2i (= 1.26 protons per nm^2) is in good agreement to the density of functional groups found for other PMO materials (=1.2 nm^{-2}).[11a] However, comparing to the theoretical amount of protons that should be present in 1 g UKON-2i (considering its molecular mass, M_w = 260.29 g mol^{-1}), it seems that only 40% of the protons are available directly. When the sulfonic acid functionality becomes diluted with non-modified, pure SiO_2, one sees that a higher ratio of the protons become available, but at the same time IEC and proton density drop (see Table 2).

It was mentioned in the introduction that porous, solid-state acids may have numerous applications, such as in fuel cells or as catalysts, or as antifouling agents. Here, we show a first proof-of-principle for the antifouling properties of the UKON nanoparticles and evidence that the strong acidity of the UKON-2i material is mandatory to maximize the (anti-) biological activity.

The potential antifouling activity of the UKON nanoparticles was evaluated as the inhibition of bacterial surface colonization on agar plates. Therefore, the opportunistic human pathogen and biofilm model organism *Pseudomonas aeruginosa* was inoculated onto agar plates and examined for its ability to grow through a barrier of nanoparticles (50 nmol), that is, from the inside of a circle of nanoparticles that had been placed onto the agar plate, to the outside (**Figure 9**). Bacterial colonies encircled by pure SiO_2 nanoparticles grew well through the barrier within 24 h, as expected, but the growth of the colonies through the barriers of UKON nanoparticles was retarded, or even prevented. In particular, UKON-2i nanoparticles showed the strongest effect on bacterial surface colonization (Figure 9). Whereas bacterial growth could be confined using UKON-2a nanoparticles for 36 h, in the case of UKON-2i the bacteria could not cross the barrier even after 48 h. Hence, these results show promise for future biological studies on the antifouling activity of UKON materials, in particular for UKON-2i.

3. Conclusion

The generation of novel high surface material with interfaces characterized by a high density of reactive organic groups paves the way towards advanced applications in various areas. In the current paper, we have concentrated on the preparation of materials with acidic properties. A novel sol–gel alkoxide silane precursor comprising benzene sulfonic acid as a bridging, organic entity was utilized for the preparation of mesoporous organosilica materials. A more refined morphology, more precisely spherical nanoparticles, was achieved via an aerosol assisted method. These nanoparticles exhibit specific surface area of up to 720 m^2 g^{-1} and pore-sizes in the range 3.5–5 nm. It could be shown that the mentioned, porous solid belong to the class of superacids with a very high surface density of 1.3×10^{18} acid

Table 2. Ion exchange capacity for UKON-2i samples.

Sample	IEC [mmol g^{-1}]	Δ_{IEC} [%][a)]	Proton density [H^+ nm^{-2}]
UKON-$2i_{100}$	1.51	40%	1.26
UKON-$2i_{50}$	0.81	43%	1.18
UKON-$2i_{10}$	0.31	81%	0.34
SiO_2	2.1×10^{-3}	-	0.002

[a)] Δ_{IEC} was obtained by dividing the experimental IEC value by the amount of protons determined by stoichiometry.

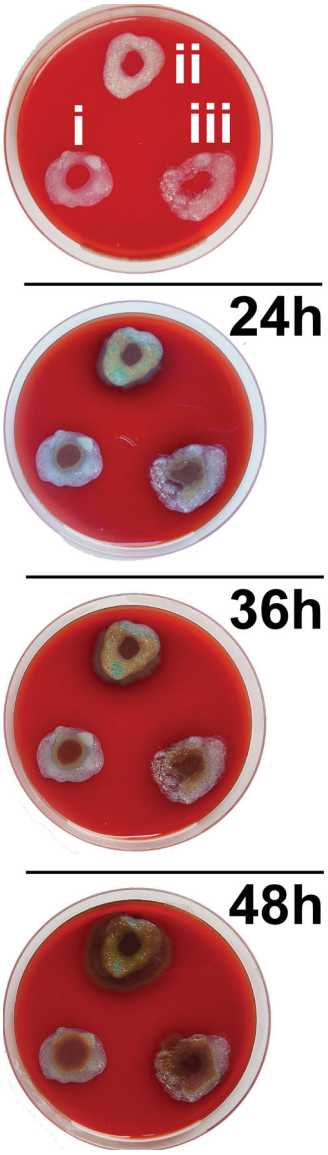

Figure 9. Representative illustration of the inhibition of bacterial surface colonization as observed on blood agar plates by the application of UKON materials as a 'barrier' surrounding the bacterial inoculum. iI) SiO_2 nanoparticles (control), iii) UKON-2a nanoparticles, and i) UKON-2i nanoparticles were applied onto the plates in a circular line and *Pseudomonas aeruginosa* was inoculated into the center of each circle (see Experimental Section). Green areas indicate bacterial growth.

groups per m^2, respectively 9.4×10^{20} surface acid groups per gram. First proof of principles experiments were performed towards antifouling applications. The comparison to materials with either none acid groups (mesoporous silica particles) or weak acidic groups (mesoporous organosilica particles containing benzoic acid) shows that only the strong solid-state acid (with the sulfonic acid) exhibit sufficient inhibition of bacterial growth. Further potential applications of the novel material reported herein are in the areas of heterogeneous catalysis of for proton conducting membranes.

4. Experimental Section

All chemicals were received from Sigma-Aldrich. Prior to use they were carefully purified and dried, when applicable. All reactions on the precursor state were performed under inert conditions using Schlenk technique. The synthesis of 1,3-bis-tri(isopropoxy)silyl-5-bromobenze (1), 1,3-bis-tri(isopropoxy)silyl-5-aniline and 3,5-bis-ti(isopropoxy) silylbenzoic acid have been described previously.[11a,b,e]

Synthesis of 1,5-bis-tri(isopropoxysilyl)-benzene-3-sulfonyl chloride (2): ^{t}BuLi (7 mL, 1.5 M, 10.6 mmol) was added dropwise to a solution of 3 g of 1,3-bis-tri(isopropoxy)silyl-5-bromobenze (7.95 mmol) in 100 mL dry Et_2O. The mixture was stirred for 30 min and then added slowly to SO_2Cl_2 in 100 mL dry Et_2O. After additional stirring for 10 min at –78 °C the solution was warmed to room temperature and the solvent was removed under vacuum. 100 mL dry pentane were added and non-soluble residues are removed via centrifugation. Finally, 1.3 g of product (2) (42%; 2.22 mmol) are obtained after vacuum distillation at 140 °C. ^{1}H NMR (400 MHz, CDCl3): δ/[ppm]: 1.19 (*d*, 36H, ^{3}J = 6.1 Hz, ^{i}Pr-CH3); 4.25 (sept, 6H, ^{3}J = 6.1 Hz, ^{i}Pr-CH); 7.74 (m, 2H, o-arom. H); 7.87 (m, 1H, p-arom. H). 13C NMR (100.61 MHz, CDCl3): δ/[ppm]: 25.6 (iPr-CH3); 65.4 (iPr-CH); 127.0 (S-arom. C); 131.9 (p-arom. C); 136.7 (o-arom. C); 141.7 (S-arom. C).

Preparation of UKON-2i Under Standard Conditions: A total of 0.5 g of precursor (2) (0.85 mmol) and structure directing agent (0.39 g Pluronic P123, or 0.21 g KLE-25) were dissolved in 1 g EtOH. 0.26 g aqueous HCl (1 M) were added dropwise while stirring. The sol was pre-hydrolized for 3 h at 60 °C and aged for 2 days at room temperature. The resulting monolithic pieces were dried at 100 °C for 24 h. Template removal occured by liquid extraction using 25 mL of H_2O and 25 mL of H_2SO4 (conc.) at 90 °C and then 25 mL EtOH and 25 mL HCl (conc.) at 60 °C within 2–4 days.

Preparation of UKON-2i Under pH Control Using Buffer Systems: The materials were prepared similar to the method described for standard conditions. However, precursor (2) and the template were dissolved in 1.5 g buffer solution.

Aerosol Synthesis of Mesoporous UKON-2a Nanoparticles: 2.84 g of 3,5-bis-ti(isopropoxy)silylbenzoic acid (5.4 mmol) were dissolved in 3.52 g EtOH. A total of 0.19 g H_2O and 2.7 µL HCl (0.1 M) were added and the solution was refluxed at 60 °C for 20 h. The sol was diluted with 7.54 g EtOH followed by addition of 0.68 g H_2O, 120 µL HCl (1 M) and 0.7 g Pluronic P123 as surfactant (pH = 2.1). The final reactant mole ratios (prec: EtOH: H_2O: HCl: P123) were 1: 44: 10: 2.022: 0.0224. The spherical mesoporous nanoparticles were obtained using an aerosol reactor (TSI Inc., Model 3076) at a volumetric flow rate of 2.6 L min^{-1}. The aerosol was dried at room temperature for 2.8 s followed by heating at 500 °C for 4.5 s and finally collected on a PTFE filter (average pore size 450 nm). The as received particles were extracted with 15 mL EtOH and 15 mL HCl conc. at 60 °C for 4 days. Full characterization occured via IR, TEM, SAXS, N_2 physisorption, and ^{13}C and ^{29}Si solid state NMR (see Supporting Information).

Aerosol Synthesis of Mesoporous UKON-2i Nanoparticles: 3.02 g of 1,5-bis-tri(isopropoxysilyl)-benzene-3-sulfonyl chloride (2) (5.14 mmol) were dissolved in 3.35 g EtOH and 0.18 g H_2O. 2.5 µL HCl (0.1 M) were added (pH = 5.2) dropwise and the solution was refluxed at 60 °C for 20 h. The sol was diluted with 7.17 g buffer solution pH 1.8 (EtOH: H_2O; 4:1) followed by 0.71 g *tetra*-butylammonium chloride (2.57 mmol) and 0.66 g Pluronic P123 as surfactant (pH = 2.1). The final reactant mole ratios (prec: EtOH: Bu_4NCl: H_2O: P123) were 1: 44: 10: 0.5: 0.0224. According to the procedure described above the spherical mesoporous nanoparticles UKON-21 are obtained by using an aerosol reactor (TSI Inc., Model 3076) and collected via a PTFE filter system. The volumetric flow rate is 1.5 L min^{-1} and the aerosol was dried at room temperature for 0.7 s followed by heating at 500 °C for 25 s. The as received particles are extracted with 15 mL EtOH and 15 mL HCl conc. at 60 °C.

Ion Exchange Capacity: To determine the ion exchange capacity (IEC) of the materials a classical titration method was used. A small amount of dried material was suspended in 0.1 M NaCl solution for 48 h. The remaining solution was titrated with 0.01 M NaOH solution in order to neutralize the exchanged proton. The IEC was calculated according to:

$$IEC = \frac{V \times M}{m} \quad (2)$$

V is the titrant volume at the equivalent point in mL; *M* is the molar concentration of the titrant (g mol^{-1}); *m* is the dried sample weight in g.

Hammett Acidity: To define the acidity strength of the acidic materials the Hammett acidity method was used. Using UV-vis technique in organic solvents the protonation state of suitable indicator dyes with different pKa values was monitored. For this purpose, p-fluoroanilin (pK_a = +2.4; weak acid), anthraquinone (pK_a = –8.2), p-fluoronitrobenzene (pK_a = –12.4), and 2,4-ninitrofluorobenzene(pK_a = –14.5) were used. The basic indicators were dissolved in dry hexane. The absorbance of the pure, non-protonated form was recorded. Then, the solid acids, Ukon-2a, Ukon-2i, and SiO2 (as reference) were added to the indicator solutions. After stirring for 30 min, the solid materials were centrifugated and the absorbance of the supernatant was measured.

Analytical Characterization: NMR-spectra were acquired on a Bruker Avance III 400 spectrometer (CDCl3 as solvent). Solid-state NMR spectra were performed on a Bruker DRX 400 spectrometer. Using a Bruker Esquire 3000 Plus spectrometer with a flow rate of 1 µg mL^{-1} the ES-MS data were recorded. The SEM images and the EDX data were received by a Zeiss 249 CrossBeam 1540XB scanning electron microscope. The Zeiss Libra 120 at 120 kv acceleration voltage performed the TEM images. FT-IR spectra were recorded by using a Perkin Elmer Spectrum 100 spectrometer using ATR unit. Small-angle X-ray scattering (SAXS) measurements were carried out with a Bruker AXS Nanostar. N2-physisorptions measurements were conducted on a Micromeritics Tristar. Acquiring a Varian Carey 100 spectrometer the as received UV/VIS spectra were recorded.

Testing the Inhibition of Bacterial Surface-Colonization: The potential antifouling activity of the UKON-2a and UKON-2i nanoparticles was tested using the bacterial biofilm model organism *Pseudomonas aeruginosa* PAO1.[54] For surface-colonization inhibition testing, the UKON material (suspended in aseptic water) was applied onto blood agar plates (Heipha) in form of a circular line, and thereafter, strain PAO1 (10 µl cell suspension of an outgrown LB-liquid culture) was inoculated to the plates at the center of the circle, in order to evaluate for the absence of growth of the bacteria from the inside to the outside of the circle during incubation (at 37 °C).

Supporting Information

Supporting Information is available from the Wiley Online Library or from the author.

Acknowledgements

The authors thank the Deutsche Forschungsgemeinschaft (DFG) for funding with in the collaborative research program SPP 1570. The authors also thank Dr. H. Schlaad (Max-Planck institute of Colloids and Interfaces) for the donation of KLE-25.

Received: July 11, 2013
Revised: September 4, 2013
Published online: October 24, 2013

[1] F. G. Omenetto, D. L. Kaplan, *Science* **2010**, *329*, 528–531.

[2] a) B. Bhushan, *Phil. Trans. Roy. Soc. A* **2009**, *367*, 1445–1486; b) P. Fratzl, *J. R. Soc. Interfaces* **2007**, *4*, 637–642.

[3] a) W. Barthlott, C. Neinhuis, *Planta* **1997**, *202*, 1–8; b) P. Roach, N. J. Shirtcliffe, M. I. Newton, *Soft Matter* **2008**, *4*, 224–240; c) A. Lafuma, D. Quere, *Nat. Mater.* **2003**, *2*, 457–460; d) R. Blossey, *Nat. Mater.* **2003**, *2*, 301–306; e) T. L. Sun, L. Feng, X. F. Gao, L. Jiang, *Acc. Chem. Res.* **2005**, *38*, 644–652; f) A. Fujishima, X. T. Zhang, D. A. Tryk, *Surf. Sci. Rep.* **2008**, *63*, 515–582.

[4] a) C. Sanchez, B. Julian, P. Belleville, M. Popall, *J. Mater. Chem.* **2005**, *15*, 3559–3592; b) D. A. Loy, K. J. Shea, *Chem. Rev.* **1995**, *95*, 1431–1442; c) U. Schubert, N. Huesing, A. Lorenz, *Chem. Mater.* **1995**, *7*, 2010–2027; d) R. J. P. Corriu, D. Leclercq, *Angew. Chem. Int. Ed.* **1996**, *35*, 1420–1436; e) R. J. P. Corriu, *Angew. Chem. Int. Ed.* **2000**, *39*, 1376–1398.

[5] a) C. T. Kresge, M. E. Leonowicz, W. J. Roth, J. C. Vartuli, J. S. Beck, *Nature* **1992**, *359*, 710–712; b) J. S. Beck, J. C. Vartuli, W. J. Roth, M. E. Leonowicz, C. T. Kresge, K. D. Schmitt, C. T. W. Chu, D. H. Olson, E. W. Sheppard, S. B. McCullen, J. B. Higgins, J. L. Schlenker, *J. Amer. Chem. Soc.* **1992**, *114*, 10834–10843; c) D. Y. Zhao, J. L. Feng, Q. S. Huo, N. Melosh, G. H. Fredrickson, B. F. Chmelka, G. D. Stucky, *Science* **1998**, *279*, 548–552; d) D. Y. Zhao, Q. S. Huo, J. L. Feng, B. F. Chmelka, G. D. Stucky, *J. Am. Chem. Soc.* **1998**, *120*, 6024–6036.

[6] F. Hoffmann, M. Cornelius, J. Morell, M. Froeba, *Angew. Chem. Int. Ed.* **2006**, *45*, 3216–3251.

[7] J. Y. Ying, C. P. Mehnert, M. S. Wong, *Angew. Chem. Int. Ed.* **1999**, *38*, 56–77.

[8] a) E. W. Abel, F. H. Pollard, P. C. Uden, G. Nickless, *J. Chromatogr.* **1966**, *22*, 23–28; b) R. K. Gilpin, M. F. Burke, *Anal. Chem.* **1973**, *45*, 1383–1389; c) U. Deschler, P. Kleinschmit, P. Panster, *Angew. Chem.* **1986**, *98*, 237–253; d) U. Schubert, N. Huesing, A. Lorenz, *Chem. Mater.* **1995**, *7*, 2010–2027; e) S. L. Burkett, S. D. Sims, S. Mann, *Chem. Commun.* **1996**, 1367–1368; f) D. J. Macquarrie, *Chem. Commun.* **1996**, 1961–1962; g) J. S. Beck, J. C. Vartuli, W. J. Roth, M. E. Leonowicz, C. T. Kresge, K. D. Schmitt, C. T. Chu, D. H. Olson, E. W. Sheppard, S. B. McCullen, J. B. Higgins, J. L. Schlenker, *J. Am. Chem. Soc.* **1992**, *114*, 10834–10843; h) P. Sutra, D. Brunel, *Chem. Commun.* **1996**, 2485–2486.

[9] a) T. Asefa, M. J. MacLachan, N. Coombs, G. A. Ozin, *Nature* **1999**, *402*, 867–871; b) S. Inagaki, S. Guan, Y. Fukushima, T. Ohsuna, O. Terasaki, *J. Am. Chem. Soc.* **1999**, *121*, 9611–9614; c) B. J. Melde, B. T. Holland, C. F. Blanford, A. Stein, *Chem. Mater.* **1999**, *11*, 3302–3308; d) B. Hatton, K. Landskron, W. Whitnall, D. Perovic, G. A. Ozin, *Acc. Chem. Res.* **2005**, *38*, 305–312.

[10] a) W. D. Wang, J. E. Lofgreen, G. A. Ozin, *Small* **2010**, *6*, 2634–2642; b) N. Mizoshita, T. Tani, S. Inagaki, **2011**, *40*, 789–800; c) F. Hoffmann, M. Froeba, *Chem. Soc. Rev.* **2011**, *40*, 608–620.

[11] a) A. Kuschel, S. Polarz, *Adv. Funct. Mater.* **2008**, *18*, 1272–1280; b) A. Kuschel, H. Sievers, S. Polarz, *Angew. Chem. Int. Ed.* **2008**, *47*, 9513–9517; c) S. Polarz, A. Kuschel, *Chem. Eur. J.* **2008**, *14*, 9816–9829; d) A. Kuschel, M. Drescher, T. Kuschel, S. Polarz, *Chem. Mater.* **2010**, *22*, 1472–1482; e) A. Kuschel, M. Luka, M. Wessig, M. Drescher, M. Fonin, G. Kiliani, S. Polarz, *Adv. Funct. Mater.* **2010**, *20*, 1133–1143; f) A. Kuschel, S. Polarz, *J. Am. Chem. Soc.* **2010**, *132*, 6558–6565; g) S. Mascotto, D. Wallacher, A. Kuschel, S. Polarz, G. A. Zickler, A. Timmann, B. M. Smarsly, *Langmuir* **2010**, *26*, 6583–6592; h) M. Wessig, M. Drescher, S. Polarz, *J. Phys. Chem.* **2013**, *117*, 2805–2816; i) M. Luka, S. Polarza, *Microporous Mesoporous Mater.* **2013**, *171*, 35–43.

[12] a) K. Schumacher, M. Gruen, K. K. Unger, *Microporous Mesoporous Mater.* **1999**, *27*, 201–206; b) A. Arkhireeva, J. N. Hay, *J. Mater. Chem.* **2003**, *13*, 3122–3127; c) I. I. Slowing , B. G. Trewyn, S. Giri, V. S. Y. Lin, *Adv. Funct. Mater.* **2007**, *17*, 1225–1236.

[13] a) K. Moller, J. Kobler, T. Bein, *Adv. Funct. Mater.* **2007**, *17*, 605–612; b) J. Kobler, K. Moeller, T. Bein, *Acs Nano* **2008**, *2*, 791–799; c) E. B. Cho, D. Kim, M. Jaroniec, *Microporous Mesoporous Mater.* **2009**, *120*, 252–256; d) S. Haffer, M. Tiemann, M. Froeba, *Chem. Eur. J.* **2010**, *16*, 10447–10452.

[14] a) Y. F. Lu, H. Y. Fan, A. Stump, T. L. Ward, T. Rieker, C. J. Brinker, *Nature* **1999**, *398*, 223–226; b) Y. F. Lu, H. Y. Fan, N. Doke, D. A. Loy,

R. A. Assink, D. A. LaVan, C. J. Brinker, *J. Am. Chem. Soc.* **2000**, *122*, 5258–5261.
[15] a) S. Guan, S. Inagaki, T. Ohsuna, O. Terasaki, *J. Am. Chem. Soc.* **2000**, *122*, 5660–5661; b) P. Mohanty, K. Landskron, *Nanoscale Res. Lett.* **2009**, *4*, 169–172; c) E.-B. Cho, D. Kim, M. Jaroniec, *Langmuir* **2007**, *23*, 11844–11849; d) E.-B. Cho, D. Kim, M. Jaroniec, *J. Phys. Chem.* **2008**, *112*, 4897–4902; e) V. Rebbin, R. Schmidt, M. Fröba, *Angew. Chem. Int. Ed.* **2006**, *45*, 5210–5214.
[16] a) J. A. Melero, R. van Grieken, G. Morales, *Chem. Rev.* **2006**, *106*, 3790–3812; b) K.-i. Shimizu, E. Hayashi, T. Hatamachi, T. Kodama, Y. Kitayama, *Tetrahedron Lett.* **2004**, *45*, 5135–5138.
[17] S. Inagaki, S. Guan, T. Ohsuna, O. Terasaki, *Nature* **2002**, *416*, 304–307.
[18] M. Sharifi, C. Kohler, P. Tolle, T. Frauenheim, M. Wark, *Small* **2011**, *7*, 1086–1097.
[19] K. Nakajima, I. Tomita, M. Hara, S. Hayashi, K. Domen, J. N. Kondo, *Adv. Mater.* **2005**, *17*, 1839.
[20] J. Alauzun, A. Mehdi, C. Reye, R. J. P. Corriu, *J. Am. Chem. Soc.* **2006**, *128*, 8718–8719.
[21] a) N. F. Hall, J. B. Conant, *J. Am. Chem. Soc.* **1927**, *49*, 3047–3061; b) G. A. Olah, G. K. S. Prakash, J. Sommer, *Science* **1979**, *206*, 13–20; c) D. Himmel, S. K. Goll, I. Leito, I. Krossing, *Angew. Chem. Int. Ed.* **2010**, *49*, 6885–6888.
[22] a) K. Arata, *Green Chemistry* **2009**, *11*, 1719–1728; b) G. D. Yadav, J. J. Nair, *Microporous Mesoporous Mater.* **1999**, *33*, 1–48.
[23] C. Mirodatos, D. Barthomeuf, *Chem. Comm.* **1981**, 39–40.
[24] A. Corma, H. Garcia, *Adv. Synth. Catal.* **2006**, *348*, 1391–1412.
[25] S. Hara, M. Miyayama, *Solid State Ionics* **2004**, *168*, 111–116.
[26] D. M. Yebra, S. Kiil, K. Dam-Johansen, *Prog. Org. Coat.* **2004**, *50*, 75–104.
[27] I. Banerjee, R. C. Pangule, R. S. Kane, *Adv. Mater.* **2011**, *23*, 690–718.
[28] H. Choi, A. C. Sofranko, D. D. Dionysiou, *Adv. Funct. Mater.* **2006**, *16*, 1067–1074.
[29] a) X. Chen, H. J. Schluesener, *Toxicol. Lett.* **2008**, *176*, 1–12; b) M. Rai, A. Yadav, A. Gade, *Biotechnol. Adv.* **2009**, *27*, 76–83.
[30] a) C. V. Bonduelle, W. M. Lau, E. R. Gillies, *ACS Appl. Mater. Interfaces* **2011**, *3*, 1740–1748; b) Y. L. Su, W. Cheng, C. Li, Z. Y. Jiang, *J. Membrane Sci.* **2009**, *329*, 246–252; c) W. Chinpa, D. Quemener, E. Beche, R. Jiraratananon, A. Deratani, *J. Membrane Sci.* **2010**, *365*, 89–97.
[31] R. Konradi, B. Pidhatika, A. Muhlebach, M. Textort, *Langmuir* **2008**, *24*, 613–616.
[32] a) K. Yoshimoto, T. Hirase, J. Madsen, S. P. Armes, Y. Nagasaki, *Macromol. Rapid. Commun.* **2009**, *30*, 2136–2140; b) C. L. Gao, G. Z. Li, H. Xue, W. Yang, F. B. Zhang, S. Y. Jiang, *Biomaterials* **2010**, *31*, 1486–1492.
[33] M. Pagliaro, R. Ciriminna, G. Palmisano, *J. Mater. Chem.* **2009**, *19*, 3116–3126.
[34] Y. Tang, J. A. Finlay, G. L. Kowalke, A. E. Meyer, F. V. Bright, M. E. Callow, J. A. Callow, D. E. Wendt, M. R. Detty, *Biofouling* **2005**, *21*, 59–71.
[35] B. Mahltig, C. Swaboda, A. Roessler, H. Bottcher, *J. Mater. Chem.* **2008**, *18*, 3180–3192.
[36] T. Hamada, O. Yonemitsu, *Synthesis-Stuttgart* **1986**, 852–854.
[37] a) J. Morell, G. Wolter, M. Froeba, *Chem. Mater.* **2005**, *17*, 804–808; b) J. Morell, M. Gungerich, G. Wolter, J. Jiao, M. Hunger, P. J. Klar, M. Froeba, *J. Mater. Chem.* **2006**, *16*, 2809–2818.
[38] C. Yoshina-Ishii, T. Asefa, N. Coombs, M. J. MacLachlan, G. A. Ozin, *Chem. Commun.* **1999**, 2539–2540.
[39] Y. Goto, S. Inagaki, *Chem. Comm.* **2002**, 2410–2411.
[40] a) A. Hakki, R. Dillert, D. W. Bahnemann, *ACS Cat.* **2013**, *3*, 565–572; b) L. Pejov, M. Ristova, B. Soptrajanov, *Spectrochim. Acta A* **2011**, *79*, 27–34; c) S. Imaizumi, H. Matsumoto, M. Ashizawa, M. Minagawa, A. Tanioka, *RSC Adv.* **2012**, *2*, 3109–3114.
[41] E. Cano-Serrano, G. Blanco-Brieva, J. M. Campos-Martin, J. L. G. Fierro, *Langmuir* **2003**, *19*, 7621–7627.
[42] S. Polarz, B. Smarsly, *J. Nanosci. Nanotech.* **2002**, *2*, 581–612.
[43] S. J. Gregg, K. S. W. Sing, *Adsorption, Surface Area and Porosity.*, Vol. *2*, 4 ed., Academic Press, London **1982**.
[44] C. G. Goeltner, B. Smarsly, B. Berton, M. Antonietti, *Chem. Mater.* **2001**, *13*, 1617–1624.
[45] E. P. Barret, L. G. Joyner, P. H. Halenda, *J. Am. Chem. Soc.* **1951**, *73*, 373–380.
[46] a)C. G. Goeltner, M. Antonietti, *Adv. Mater.* **1997**, *9*, 431; b) M. Antonietti, B. Berton, C. Goeltner, H. P. Hentze, *Adv. Mater.* **1998**, *10*, 154.
[47] a) C. G. Goeltner, B. Berton, E. Kraemer, M. Antonietti, *Chem. Commun.* **1998**, 2287–2288; b) T. Brezesinski, C. Erpen, K. Iimura, B. Smarsly, *Chem. Mater.* **2005**, *17*, 1683–1690; c) T. Brezesinski, A. Fischer, K. Iimura, C. Sanchez, D. Grosso, M. Antonietti, B. M. Smarsly, *Adv. Funct. Mater.* **2006**, *16*, 1433–1440; d) M. Thommes, B. Smarsly, M. Groenewolt, P. I. Ravikovitch, A. V. Neimark, *Langmuir* **2006**, *22*, 756–764; e) D. Fattakhova-Rohlfing, M. Wark, T. Brezesinski, B. M. Smarsly, J. Rathousky, *Adv. Funct. Mater.* **2007**, *17*, 123–132.
[48] S. Foerster, C. Burger, *Macromolecules* **1998**, *31*, 879.
[49] V. Rebbin, M. Jakubowski, S. Potz, M. Froeba, *Microporous Mesoporous Mater.* **2004**, *72*, 99–104.
[50] a) C. J. Brinker, Y. F. Lu, A. Sellinger, H. Y. Fan, *Adv. Mater.* **1999**, *11*, 579-+; b) G. V. R. Rao, G. P. Lopez, J. Bravo, H. Pham, A. K. Datye, H. F. Xu, T. L. Ward, *Adv. Mater.* **2002**, *14*, 1301.
[51] Y. Xiong, S. E. Pratsinis, *J. Aerosol. Sci.* **1991**, *22*, 637–655.
[52] a) L. P. Hammett, A. J. Deyrup, *J. Am. Chem. Soc.* **1932**, *54*, 2721–2739; b) C. Paze, S. Bordiga, C. Lamberti, M. Salvalaggio, A. Zecchina, G. Bellussi, *J. Phys. Chem.* **1997**, *101*, 4740–4751; c) S. H. Chai, H. P. Wang, Y. Liang, B. Q. Xu, *Green Chem.* **2007**, *9*, 1130–1136; d) F. Shirini, M. Mamaghani, M. Seddighi, *Catal. Commun.* **2013**, *36*, 31–37.
[53] a)A. Bhaumik, S. Inagaki, *J. Am. Chem. Soc.* **2001**, *123*, 691–696; b) V. Ganesan, A. Walcarius, *Langmuir* **2004**, *20*, 3632–3640; c) R. K. Nagarale, G. S. Gohil, V. K. Shahi, R. Rangarajan, *Macromol.* **2004**, *37*, 10023–10030.
[54] D. Schleheck, N. Barraud, J. Klebensberger, J. S. Webb, D. McDougald, S. A. Rice, S. Kjelleberg, *PloS One* **2009**, *4*.